ATRP Synthesis of Thermally Responsive Molecular Brushes from Oligo(ethylene oxide) Methacrylates

Shin-ichi Yamamoto, Joanna Pietrasik,† and Krzysztof Matyjaszewski*

Center for Macromolecular Engineering, Department of Chemistry, Carnegie Mellon University, 4400 Fifth Avenue, Pittsburgh, Pennsylvania 15213

Received August 31, 2007; Revised Manuscript Received October 18, 2007

ABSTRACT: Molecular brushes consisting of statistical copolymers of di(ethylene glycol) methyl ether methacrylate (MEO_2MA) and tri(ethylene glycol) methyl ether methacrylate (MEO_3MA) were synthesized by grafting from poly(2-(2-bromoisobutyryloxy)ethyl methacrylate (PBIEM) macroinitiators using atom transfer radical polymerization (ATRP) providing copolymers with controlled composition and molecular weights ranging from M_n = 601 500 to 2 731 000 with polydispersity indexes (M_w/M_n) between 1.06 and 1.20. The lower critical solution temperature (LCST) of the brushes increased with the mole fraction of MEO_3MA in the side chain, and the hysteresis between the heating and cooling cycles decreased with the length of the side chain. Brush copolymers with different graft density were also prepared, and the average hydrodynamic diameter, measured by dynamic light scattering (DLS), varied with temperature above the LCST, and the maximum diameter of the aggregates increased according to the graft density of side chain along the brush backbone. These two monomers were also incorporated into side chain block copolymer brushes by ATRP. The cloud point of the block brushes solution displayed two stages of aggregation during heating, exhibiting the results of both intermolecular and intramolecular aggregation. This behavior was strongly dependent on the sequence of the side chain segments. As the temperature increased, particles consisting of collapsed $PMEO_2MA$ and $PMEO_3MA$ segments aggregated upon further heating to precipitate as larger particles.

Introduction

Stimuli-responsive polymers have been extensively investigated for the development of smart materials for various applications.[1−6] Diverse types of stimuli, such as temperature, pH, or light, can affect the properties and conformation of polymer chains.[7,8] Thermoresponsive, water-soluble polymers exhibiting a lower critical solution temperature (LCST) in water have been increasingly investigated for nanotechnology and biotechnology applications.[9,10] A variety of applications, including phase separation immunoassays,[11] hyperthermia-induced drug delivery,[12] and environmentally responsive Pickering emulsions,[13] have been reported. Poly(*N*-isopropylacrylamide) (PNIPAM), which displays a LCST in water around 32 °C, has been the most studied thermoresponsive polymer targeting biological applications.[14] In addition, new thermoresponsive water-soluble polymers were developed by the introduction of nonionizable hydrophilic moieties, such as oligo(ethylene oxide) groups, into copolymers. Poly(ethylene glycol) (PEG) is an uncharged, water-soluble, nontoxic polymer used to prepare biocompatible materials, such as biosensors and drug delivery systems.[15,16] Living cationic, anionic, and radical polymerizations were used to prepare thermoresponsive polymers containing oligo(ethylene oxide) side chains.[17−31] Recently, Lutz and co-workers carried out the copolymerization of di(ethylene glycol) methyl ether methacrylate (MEO_2MA) with poly(ethylene glycol) methyl ether methacrylate (MW = 475) (PEGMA) by atom transfer radical polymerization (ATRP).[19] The LCST of obtained polymer increased with the composition of PEGMA. Also, Huck and co-workers investigated collapse transition of this copolymer grafted from silicon surface upon heating by the measurements of equilibrium contact angle by AFM.[31]

Densely grafted copolymers, also known as molecular bottle brushes, are the subject of continuing interest mainly due to their unusual architecture and properties.[32,33] A molecular bottle brush consists of a flexible backbone with a high density of side chains along the backbone separated by a distance much smaller than their unperturbed dimensions. This leads to significant congestion and entropically unfavorable chain extension of the backbone and side chains, which prevents the polymer from adopting a random coil conformation. Conformation behavior of molecular brushes in solution and at interfaces have been studied theoretically and experimentally.[34] ATRP is one of the most robust controlled/living radical polymerization (CRP) techniques, and suitable for the synthesis of multifunctional macromolecules, since the low radical concentrations present during the polymerizations reduce the contribution of inter- and intramolecularly terminated chains.[35−44] This is especially important for the preparation of densely grafted copolymers with a multiplicity of chains in the vicinity of the polymer backbone to limit the propensity for cross-linking when intermolecular termination occurs between multifunctional (co)polymers. Because of the wide range of monomers that can be polymerized by ATRP, molecular brushes with interesting solution properties can be envisioned.[45−48]

Recently, we reported the synthesis of thermoresponsive copolymer brushes containing 2-(dimethylamino)ethyl methacrylate monomer units in the side chains.[49] A temperature-induced coil collapse of single molecular brush macromolecules with poly(*N*-isopropylacrylamide) side chains was also reported.[50] Here we report the synthesis and characterization of statistical and block copolymer brushes of di(ethylene glycol) methyl ether methacrylate (MEO_2MA) and tri(ethylene glycol) methyl ether methacrylate (MEO_3MA) prepared by ATRP using CuBr/4,4′-dinonyl-2,2′-bipyridine (dNbpy) as the catalyst. The

* Corresponding author. E-mail: km3b@andrew.cmu.edu.
† Current address: Technical University of Lodz, Institute of Polymer and Dye Technology, Stefanowskiego 12/16, 90-924 Lodz, Poland.

10.1021/ma701970t CCC: $37.00
Published on Web 12/01/2007

Scheme 1

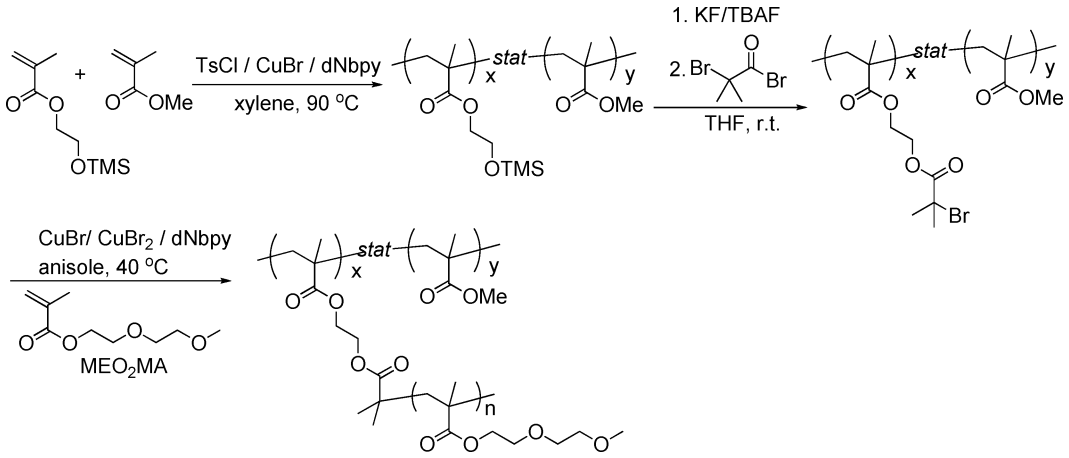

cloud point of these brush molecules solution is strongly dependent on the composition and architecture of the copolymer side chains.

Experimental Section

Materials. All chemicals were purchased from Aldrich or Acros and used as received unless otherwise stated. Methyl methacrylate (MMA), di(ethylene glycol) methyl ether methacrylate (MEO_2MA), and 2-(trimethylsilyloxy)ethyl methacrylate (HEMA-TMS) were purified by vacuum distillation before use. Copper(I) bromide (Aldrich, 98+%) was purified by stirring with glacial acetic acid, followed by filtration and washing the solids with ethanol (three times) and diethyl ether (two times). Tri(ethylene glycol) methyl ether methacrylate (MEO_3MA) was prepared by the previously reported procedure.[18]

Analysis. Apparent molecular weight and molecular weight distribution were measured using GPC (Waters Microstyragel columns (guard, 10^2, 10^3, and 10^5 Å), THF eluent at 35 °C, flow rate = 1.00 mL/min). The detectors consisted of a differential refractometer (Waters 410, λ = 930 nm) and a multiangle laser light scattering (MALLS) detector (Wyatt Technology DAWN EOS, 30 mW, λ = 690 nm). The apparent molecular weights were determined with a calibration based on poly(methyl methacrylate) (PMMA) standards using GPCWin software from Polymer Standards Service. Absolute molecular weights were determined with the d*n*/d*c* values of 0.023 using Wyatt ASTRA software. Conversions were determined by gas chromatography (GC) using a Shimadzu GC-14A gas chromatograph equipped with a FID detector and ValcoBond 30 m VB WAX Megabore column. ^{1}H NMR spectra of copolymers were examined in $CDCl_3$ at 30 °C using a Bruker Advance 300 MHz spectrometer. UV−vis spectra were recorded using a Varian Cary 7 Bio UV−vis spectrophotometer equipped with a digital temperature controller. The wavelength of 600 nm was used for the determination of the cloud point. The range of temperatures was from 20 to 60 °C, and heating and cooling rates were 1 °C/min; the temperature onset of loss of transmittance on heating cycle was defined as a cloud point. The particle size was measured using dynamic light scattering (DLS) (high-performance particle sizer, model HPP5001, Malvern Instruments). Measurements were taken from 20 to 55 °C at 1.0 °C intervals.

Synthesis. Poly(2-(2-bromoisobutyryloxy)ethyl methacrylate) (PBIEM) and poly(2-(2-bromoisobutyryloxy)ethyl methacrylate-*stat*-methyl methacrylate) P(BIEM-*stat*-MMA) were prepared as previously reported.[45]

General Procedure for the Preparation of Poly(2-(2-bromoisobutyryloxy)ethyl Methacrylate)-*graft*-(Di(ethylene glycol) Methyl Ether Methacrylate)) (PBIEM-*g*-$PMEO_2MA$) (B1). 0.025 g (0.06 mmol) of dNbpy, 0.67 mg (0.003 mmol) of $CuBr_2$, 7.60 mg (0.03 mmol −Br) of PBIEM (M_n = 34 000, M_w/M_n = 1.05), 2.82 g (15 mmol) of MEO_2MA, and 2.4 mL of anisole were added to a 25 mL Schlenk flask, and oxygen was removed by subjecting the contents of the flask to three freeze−pump−thaw cycles. Next, 3.86 mg (0.027 mmol) of CuBr was added under nitrogen flow. The stirred flask was placed in an oil bath controlled at 40 °C. Samples were withdrawn periodically to monitor monomer conversion (GC) and evolution of molecular weight (GPC). The polymerization was stopped by opening the flask and exposing the contents to air. The reaction mixture was diluted with THF and passed through an alumina column to remove the catalyst. The polymer was precipitated by adding the solution to hexane, filtering, and drying under high vacuum, yielding a polymer with M_n = 435 000 and M_w/M_n = 1.10. Other brushes containing homopolymer or statistical copolymer as a side chain (**B2**−**B10**) were also prepared using the same procedure.

Poly(2-(2-bromoisobutyryloxy)ethyl Methacrylate)-*graft*-(Poly-(di(ethylene glycol) Methyl Ether Methacrylate)-*block*-Poly(tri-(ethylene glycol) Methyl Ether Methacrylate)) (PBIEM-*g*-($PMEO_2MA$-*b*-$PMEO_3MA$)) (B11). 0.025 g (0.06 mmol) of dNbpy, 0.67 mg (0.003 mmol) of $CuBr_2$, 7.80 mg (0.03 mmol −Br) of PBIEM-*g*-$PMEO_2MA$ (M_n = 364 400, M_w/M_n = 1.11), 3.48 g (15 mmol) of MEO_3MA, and 2.4 mL of acetone were added to a 25 mL Schlenk flask, and oxygen was removed by subjecting the contents of the flask to three freeze−pump−thaw cycles. Next, 12.8 mg (0.09 mmol) of CuBr was added under nitrogen flow. The stirred flask was placed in an oil bath controlled at 40 °C; samples were withdrawn periodically to monitor monomer conversion (GC) and evolution of molecular weight (GPC). The polymerization was stopped by opening the flask and exposing the contents to air. The reaction mixture was diluted with THF and passed through an alumina column to remove the catalyst. The polymer was precipitated by adding the solution to hexane, filtering, and drying under high vacuum, yielding a polymer with M_n = 604 000 and M_w/M_n = 1.21. Other brushes containing block copolymer side chain (**B12** and **B13**) were also prepared using the same procedure.

Results and Discussion

Homopolymerization and Statistical Copolymerization. We previously reported the synthesis of molecular brushes consisting poly(oligo(ethylene oxide) methacrylate (M_w = 300) units in the side chain,[51] but there has been no report investigating the thermal response of these brushes. Initially, we investigated homopolymerization of MEO_2MA by ATRP using several different macroinitiators (Scheme 1).

PBIEM and PBIEM-*stat*-MMA macroinitiators (**M1**−**M4**) were synthesized according to the previous reports (Table 1). The molar fraction of initiation site was estimated by ^{1}H NMR spectroscopy.

The results of the grafting from polymerizations of MEO_2-MA are listed in Table 2. The polymerizations were carried out at 40 °C in anisole, in the presence of PBIEM (**M1**) macroini-

Table 1. Characterization of P(BIEM-*stat*-MMA) Macroinitiator

macro-initiator	DP[a]	$M_{n,app}$[b]	M_w/M_n[b]	fraction of initiator groups[a]	no. of initiator groups per chain[c]
M1	127	34 000	1.05	100	117
M2	246	65 800	1.11	100	226
M3	268	43 300	1.11	30	56
M4	238	48 000	1.08	53	87
M5	290	61 600	1.07	76	142

[a] Determined by conversion from GC. [b] Apparent molecular weights were determined by GPC in THF with PMMA calibration. [c] Determined by ^{1}H NMR.

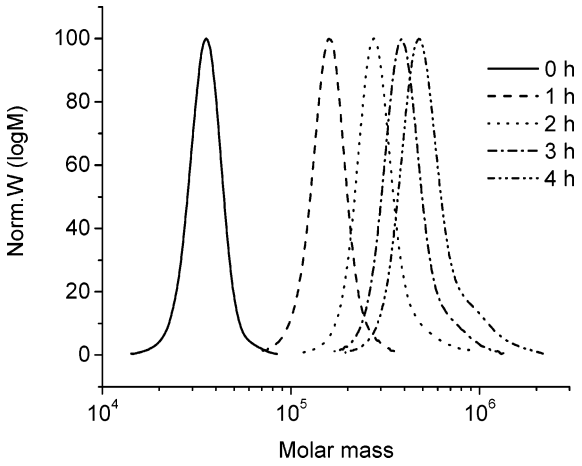

Figure 1. GPC traces of graft polymerization of MEO_2MA. Conditions: $[MEO_2MA]_0/[PBIEM]_0/[CuBr]_0/[CuBr_2]_0/[dNbpy]_0 = 500/1/0.9/0.1/2$.

tiator, copper(I) bromide/dNbpy as catalyst, and 10 mol % $CuBr_2$ as a deactivator (**B1**). Several samples of $PMEO_2MA$ brushes with different length of side chains were prepared. In every case, the graft polymerization of MEO_2MA was well controlled, resulting in the synthesis of polymers with low PDI (**B2** and **3**). Apparent molecular weight measured by GPC was much lower than the MW measured by GPC-MALLS because their highly compact nature does not correspond well to the linear standards. GPC traces are shown in Figure 1. GPC traces shifted clearly to the higher molecular region with monomer conversion while retaining narrow molecular weight distribution. The polymerization was also conducted using P(BIEM-*stat*-MMA) macroinitiators to obtain the corresponding brushes with low PDI (**B4**−**B6**). The polymerization proceeded in a controlled manner, similar to the case of **M1**.

The homopolymerization of MEO_3MA and statistical copolymerization of MEO_2MA with MEO_3MA were investigated using **M1** as a macroinitiator (Scheme 2). These results are shown in Table 3.

The graft polymerization of MEO_3MA, using the same catalyst, was also well controlled, yielding $PMEO_3MA$ brush macromolecules with low M_w/M_n (**B7**). Furthermore, a graft copolymerization was carried out using MEO_2MA and MEO_3MA as comonomers to obtain the brushes consisting of P(MEO_2MA-*stat*-MEO_3MA) as side chains (Scheme 2). The copolymerization was conducted with three different comonomer feed ratios under similar conditions (**B8**−**B10**). In every case, the polymerization resulted in brushes consisting P(MEO_2MA-*stat*-MEO_3MA) copolymers as side chains with low M_w/M_n. The compositions of side chains were estimated using ^{1}H NMR spectroscopy. The mole fractions of the comonomers in the final brushes were very close to the monomer feed ratio.

Block Copolymerization. Brush copolymers with blocks of MEO_2MA with MEO_3MA in the side chain were prepared to examine the effect of segment length and sequence of the blocks in the side chain on LCST behavior. Details of reaction conditions, and properties of the resulting copolymers, are listed in Table 4. The first graft polymerization was carried out using **M2** as a macroinitiator. Chain extension was examined using the same catalyst, but acetone was used as the solvent instead of anisole because the first brush was poorly soluble in pure anisole. The GPC traces are shown in Figure 2. The GPC trace of the block copolymer clearly shifted to the higher molecular region while retaining low PDI.

Thermal Properties of Homopolymer and Statistical Copolymer. Transmittance of aqueous solutions of the $PMEO_2$-MA brushes was measured using a UV spectrometer in order to determine the dependence of the thermal properties on temperature. The transmittance of 0.3 wt % aqueous solution of the polymer was monitored at 600 nm at a heating or cooling rate of 1.0 °C min^{-1}. All of the solutions started to become cloudy around 22 °C, which is slightly lower than linear $PMEO_2$-MA (26 °C).[18,19,52] Subsequently, the transmittance dropped to 0%. This change was reversible and similar to the case of a homopolymer of $PMEO_2MA$. The effect of the increasing the length of the side chains is shown in Figure 3. Aqueous solutions of all of the brushes clouded at 22.5 °C during the heating cycle. However, the hysteresis between the heating and cooling cycle decreased with increasing length of side chain, suggesting that the $PMEO_2MA$ side chains cannot efficiently disaggregate close to the PBIEM backbone due to steric hindrance. Therefore, the polymer having short side chains needs longer time to dissolve.

The effect of the side chain density on the thermal properties of the brushes (**B4**−**B6**) was also studied by DLS (Figure 4). In every case, the apparent diameter of the aggregate increased rapidly around the LCST and decreased upon further heating. This behavior is very similar to the linear polymer containing poly(ethylene oxide) side chains.[30,52] The maximum diameter of the aggregate increased with the graft density of the side chains. This tendency indicates that the aggregation of $PMEO_2$-MA brushes more closely resembles the case of the linear homopolymer as the density of initiation sites on the macroinitiator decreases. These results suggest that the LCST of brushes is determined by the structure of the side chain. The diameter of the particle formed by aggregation above LCST increases with the grafting density and with total molecular weight.

Table 2. Conversion and Molecular Weight Data of $PMEO_2MA$ Initiated from PBIEM[a]

entry	macroinitiator	time (h)	DP_{conv}[b]	$M_{n,theo}$[b]	$M_{n,app}$[c]	$M_{n,absolute}$[d]	M_w/M_n[d]
B1	**M1**	1	25	648 000	165 000	602 000	1.06
B2	**M1**	2	50	1 261 000	267 000	1 299 000	1.08
B3	**M1**	4	115	2 783 000	435 000	2 457 000	1.12
B4	**M3**	3	90	1 377 000	522 000	1 935 000	1.20
B5	**M4**	4	120	2 549 000	626 000	2 407 000	1.18
B6	**M5**	3	100	3 559 000	586 000	2 667 000	1.14

[a] Conditions: $[MEO_2MA]_0/[In]_0/[CuBr]_0/[CuBr_2]_0/[dNbpy]_0 = 500/1/0.9/0.1/2$ in anisole solution (40 vol %). [b] Calculated from conversion measured by GC. [c] Determined by GPC in THF with PMMA calibration. [d] Determined by GPC MALLS in THF.

Scheme 2

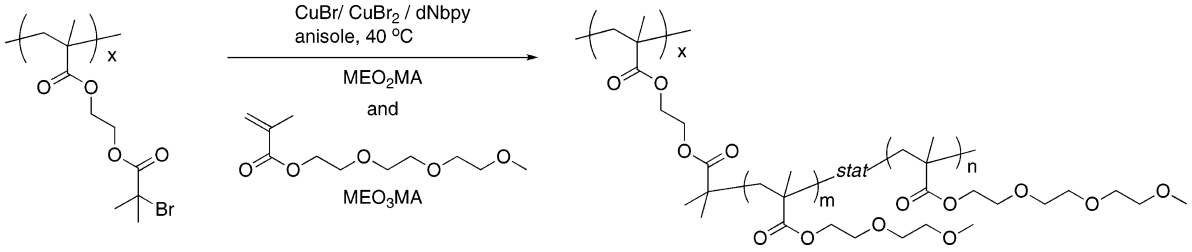

Table 3. Conversion and Molecular Weight Data of Graft Copolymerization of MEO_2MA with MEO_3MA[a]

entry	$[MEO_2MA]_0/[MEO_3MA]_0$	DP_{conv}[b]	$M_{n,theo}$[b]	$M_{n,app}$[c]	$M_{n,absolute}$[d]	M_w/M_n[c]	composition[e] (m/n)
B7	0/500	90	2 992 000	489 000	2 731 000	1.09	0/100
B8	125/375	100	2 920 000	523 000	2 898 000	1.11	38/62
B9	250/250	85	2 366 000	437 000	2 544 000	1.12	58/42
B10	375/125	95	2 472 000	621 000	2 004 000	1.11	78/22

[a] Conditions: For **M1** (M_n = 34 000 g/mol, M_w/M_n = 1.05, DP = 127), $[monomers]_0/[In]_0/[CuBr]_0/[CuBr_2]_0/[dNbpy]_0$ = 500/1/0.9/0.1/2 in anisole solution (40 vol %). [b] Calculated from conversion measured by GC. [c] Determined by GPC in THF with PMMA calibration. [d] Determined by GPC MALLS in THF. [e] Determined by ^1H NMR.

Table 4. Conversion and Molecular Weight Data for the Block Copolymerization of MEO_2MA with MEO_3MA[a]

	first block[a]					second block[b]					
entry	monomer	DP_{conv}[c]	$M_{n,theo}$[c]	$M_{n,app}$[d]	M_w/M_n[d]	monomer	DP_{conv}[c]	$M_{n,theo}$[c]	$M_{n,app}$[d]	M_w/M_n[d]	composition[e] (m/n)
B11	MEO_2MA	55	2 307 000	454 000	1.21	MEO_3MA	20	3 354 000	549 000	1.25	65/35
B12	MEO_2MA	25	1 128 000	364 000	1.11	MEO_3MA	55	4 008 000	604 000	1.21	22/78
B13	MEO_3MA	35	1 898 000	416 000	1.10	MEO_2MA	50	4 020 000	747 000	1.23	73/27

[a] Conditions: For **M2** (M_n = 65 800 g/mol, M_w/M_n = 1.11, DP = 246), $[monomer]_0/[In]_0/[CuBr]_0/[CuBr_2]_0/[dNbpy]_0$ = 500/1/0.9/0.1/2 in anisole solution (40 vol %) at 40 °C. [b] Conditions: $[monomer]_0/[In]_0/[CuBr]_0/[CuBr_2]_0/[dNbpy]_0$ = 500/1/0.9/0.1/2 in acetone solution (40 vol %) at 40 °C. [c] Calculated from conversion measured by GC. [d] Determined by GPC in THF with PMMA calibration. [e] Determined by ^1H NMR.

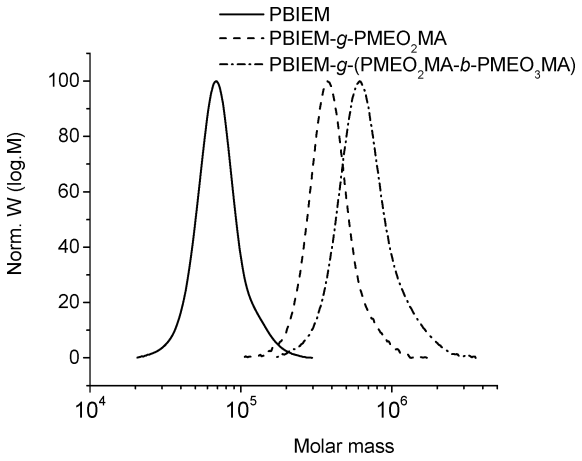

Figure 2. GPC traces of block copolymerization of MEO_2MA with MEO_3MA from PBIEM (**B12**).

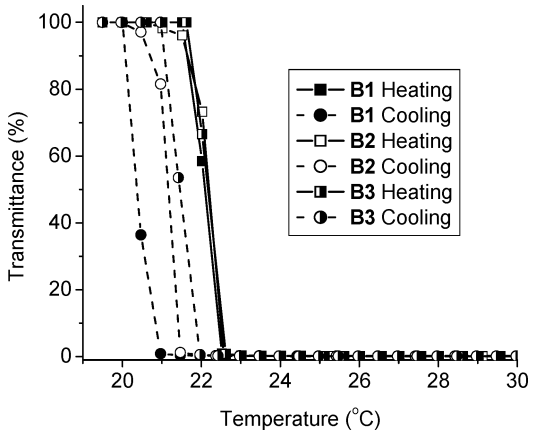

Figure 3. Effect of the side chain length on temperature dependence of optical transmittance changes at 600 nm for PBIEM-*graft*-$PMEO_2$-MA aqueous solution.

The effect of the molar ratio of comonomers in the statistical copolymer side chains on LCST was also studied (Figure 5). All changes were thermally reversible, but a small hysteresis (~2 °C) was observed between the heating and cooling cycles. The LCST of **S7,** with $PMEO_3MA$ side chains, was about 45 °C, which is slightly lower than linear $PMEO_3MA$ (51 °C).[18,52] The relationship between the LCST and the composition of the copolymer is shown in Figure 6. The measured LCST values increased with increasing percentage of MEO_3MA in the $PMEO_2MA$-*stat*-$PMEO_3MA$ side chain. These results are similar to that of linear $PMEO_2MA$-*stat*-$PMEO_3MA$.

Thermal Properties of Block Copolymer. Light transmittance through solutions of the brushes consisting of side chain block copolymers of MEO_2MA and MEO_3MA were measured using UV spectrometry in order to determine the dependence of the thermal properties on temperature (Figure 7). In the case of **B12**, where the sequence was $PMEO_2MA$-*b*-$PMEO_3MA$, the cloud point was around 50 °C, which is higher than the temperature predicted from the statistical copolymer brush with the same composition (ca. 40 °C). On the other hand, the solution of **B13,** $PMEO_3MA$-*b*-$PMEO_2MA$, started to cloud at ca. 26 °C, which corresponds to the LCST of $PMEO_2MA$, and then the curve of transmittance displayed a plateau around 30 °C. Finally, the solution restarted to cloud rapidly ca. 40 °C. However, the % transmittance in the cooling cycle was constant until ca. 30 °C, and then it increased rapidly around 28 °C.

This suggests that in the case of sample **B12** the inner $PMEO_2MA$ segments aggregate to form small micelles at its intrinsic LCST, but the brush remains water-soluble, since it is held in solution by the hydrophilic nonaggregated $PMEO_3MA$ segments. We observed a similar behavior in the case of the block copolymer of linear $PMEO_2MA$ with $PMEO_3MA$.[52] On

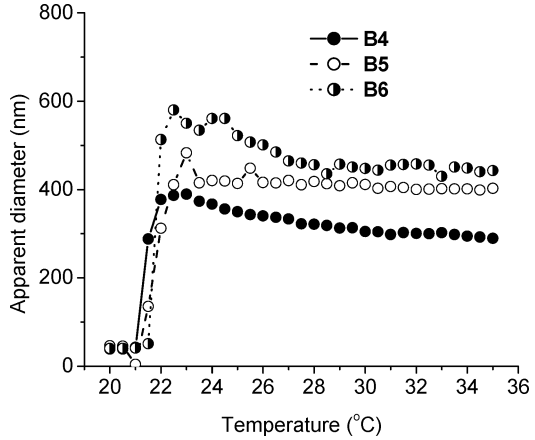

Figure 4. Temperature dependence of hydrodynamic diameter change for 0.3 wt % aqueous solution of $PMEO_2MA$ brushes.

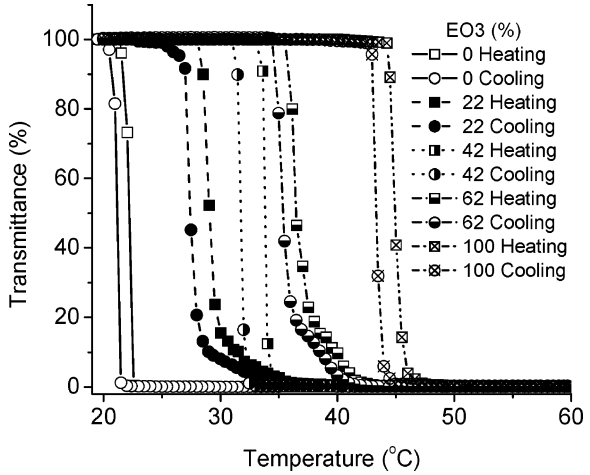

Figure 5. Effect of the composition in statistical copolymer of MEO_2-MA with MEO_3MA on optical transmittance changes at 600 nm for 0.3 wt % of aqueous solution.

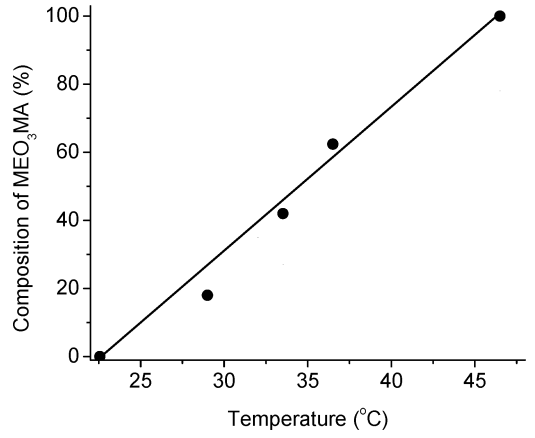

Figure 6. Relationship between LCST determined in heating cycle for 0.3 wt % aqueous solutions of the copolymers and % composition of MEO_3MA in the brushes.

the other hand, sample **B13** could precipitate by the aggregation of outer $PMEO_2MA$ segments at 26 °C, and then the $PMEO_3$-MA segments located on the inside of the brush aggregate around the LCST of $PMEO_3MA$ on continued heating. While in the cooling cycle, $PMEO_3MA$ segments disaggregated around the intrinsic LCST of $PMEO_3MA$, and the $PMEO_2MA$ segments remain aggregated. Therefore, the % transmittance of the solution remained low until the shell disaggregated at 26 °C,

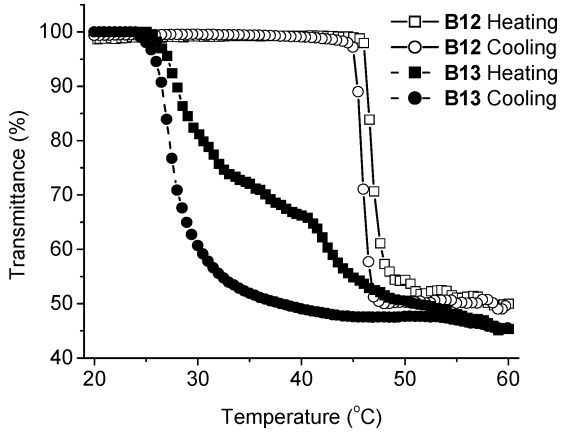

Figure 7. Temperature dependence of optical transmittance change for 0.3 wt % aqueous solution of block brushes. Solid curve: PBIEM-*g*-($PMEO_2MA$-*b*-$PMEO_3MA$) (**B12**). Dashed curve: PBIEM-*g*-($PMEO_3$-MA-*b*-$PMEO_2MA$) (**B13**).

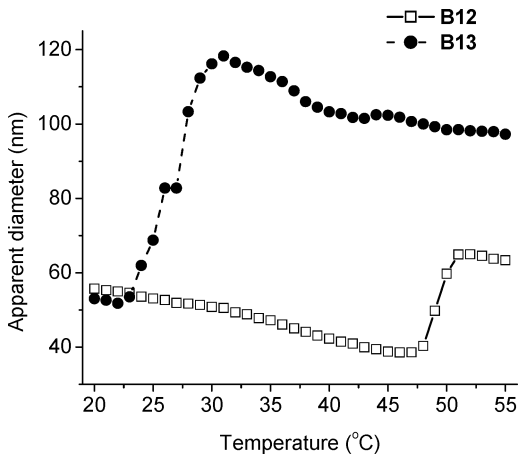

Figure 8. Temperature dependence of hydrodynamic diameter change for 0.3 wt % aqueous solution of block brushes. Solid curve: PBIEM-*g*-($PMEO_2MA$-*b*-$PMEO_3MA$) (**B12**). Dashed curve: PBIEM-*g*-($PMEO_3$-MA-*b*-$PMEO_2MA$) (**B13**).

corresponding to the LCST of $PMEO_2MA$ reaching 100% transmittance.

The change of *Z*-average hydrodynamic diameter of thermo-responsive polymer particles was also measured (Figure 8). In the case of **B12**, the diameter of the brush started to decrease at 20 °C, reaching a minimum at 45 °C, and then the diameter increased upon further heating. While in the case of **B13**, the diameter started to increase at 23 °C, reaching a maximum at 31 °C, and then decreased with further increase in temperature. These results suggest that the $PMEO_2MA$ segment inside of the block−brush copolymer, **B12**, aggregated around 25 °C by intramolecular aggregation, but $PMEO_3MA$ segments in the outer shell of the brush behaved as a water-soluble corona. The $PMEO_2MA$ segment located on the outside of **B13** aggregated around their LCST to form a shell. These vesicles assembled by intermolecular aggregation. Then, the vesicles shrank by internal aggregation of the $PMEO_3MA$ core segments upon further heating.

Conclusion

Molecular brushes consisting of statistical and block copolymers of MEO_2MA with MEO_3MA in the side chains were prepared by Cu-based ATRP. Well-defined brushes with predictable molecular weights and low M_w/M_n were formed. The thermal properties of aqueous solutions of the brushes were

studied by UV−vis and DLS. The LCST values determined for the brushes scaled linearly with the composition of the statistical side chain. Upon heating, the brush with $PMEO_2MA$-*b*-PME_3-MA sequence in the side chain formed micelles consisting of collapsed $PMEO_2MA$ segments and soluble $PMEO_3MA$ chains as core and corona, respectively. Upon further heating the size of particles progressively increased, even above the cloud point observed by UV−vis. On the other hand, brush molecules with $PMEO_3MA$-*b*-$PMEO_2MA$ side chains formed vesicles consisting of aggregated $PMEO_2MA$ shell segments and soluble $PMEO_3MA$ core segments.

Acknowledgment. The authors are grateful for the financial support provided by the National Science Foundation (DMR-0549353 and 0733135) and members of the CRP Consortium at Carnegie Mellon University (CMU).

References and Notes

(1) Miyata, T. *Supramol. Des. Biol. Appl.* **2002**, 191−225.
(2) Gil, E. S.; Hudson, S. M. *Prog. Polym. Sci.* **2004**, *29*, 1173−1222.
(3) Brittain, W. J.; Boyes, S. G.; Granville, A. M.; Baum, M.; Mirous, B. K.; Akgun, B.; Zhao, B.; Blickle, C.; Foster, M. D. *Adv. Polym. Sci.* **2006**, *198*, 125−147.
(4) Sukhorukov, G.; Fery, A.; Moehwald, H. *Prog. Polym. Sci.* **2005**, *30*, 885−897.
(5) Tanaka, Y.; Gong, J. P.; Osada, Y. *Prog. Polym. Sci.* **2005**, *30*, 1−9.
(6) Dobrynin, A. V.; Rubinstein, M. *Prog. Polym. Sci.* **2005**, *30*, 1049−1118.
(7) Lokuge, I. S.; Bohn, P. W. *Langmuir* **2005**, *21*, 1979−1985.
(8) Traitel, T.; Kost, J. *Adv. Exp. Med. Biol.* **2004**, *553*, 29−43.
(9) Schmaljohann, D. *Adv. Drug Delivery Rev.* **2006**, *58*, 1655−1670.
(10) Ichijo, H.; Kishi, R. *Springer Ser. Mater. Sci.* **1999**, *35*, 71−83.
(11) Kulkarni, S.; Schilli, C.; Mueller, A. H. E.; Hoffman, A. S.; Stayton, P. S. *Bioconjugate Chem.* **2004**, *15*, 747−753.
(12) Han, H. D.; Choi, M. S.; Hwang, T.; Song, C. K.; Seong, H.; Kim, T. W.; Choi, H. S.; Shin, B. C. *J. Pharm. Sci.* **2006**, *95*, 1909−1917.
(13) Santos, A. M.; Elaissari, A.; Martinho, J. M. G.; Pichot, C. *Polymer* **2005**, *46*, 1181−1188.
(14) Schild, H. G. *Prog. Polym. Sci.* **1992**, *17*, 163−249.
(15) Duncan, R. *Nat. Rev. Drug Discovery* **2003**, *2*, 347−360.
(16) Pasut, G.; Veronese, F. M. *Adv. Polym. Sci.* **2006**, *192*, 95−134.
(17) Aoshima, S.; Sugihara, S.; Shibayama, M.; Kanaoka, S. *Macromol. Symp.* **2004**, *215*, 151−163.
(18) Han, S.; Hagiwara, M.; Ishizone, T. *Macromolecules* **2003**, *36*, 8312−8319.
(19) Lutz, J.-F.; Hoth, A. *Macromolecules* **2006**, *39*, 893−896.
(20) Li, D.; Jones, G. L.; Dunlap, J. R.; Hua, F.; Zhao, B. *Langmuir* **2006**, *22*, 3344−3351.
(21) Hua, F.; Jiang, X.; Li, D.; Zhao, B. *J. Polym. Sci., Part A: Polym. Chem.* **2006**, *44*, 2454−2467.
(22) Mertoglu, M.; Garnier, S.; Laschewsky, A.; Skrabania, K.; Storsberg, J. *Polymer* **2005**, *46*, 7726−7740.
(23) Ali, M. M.; Stover, H. D. H. *J. Polym. Sci., Part A: Polym. Chem.* **2005**, *44*, 156−171.
(24) He, L.; Huang, J.; Chen, Y.; Liu, L. *Macromolecules* **2005**, *38*, 3351−3355.
(25) Hu, F.; Neoh, K. G.; Cen, L.; Kang, E.-T. *Biomacromolecules* **2006**, *7*, 809−816.
(26) Sugihara, S.; Ohashi, M.; Ikeda, I. *Macromolecules* **2007**, *40*, 3394−3401.
(27) Terashima, T.; Ouchi, M.; Ando, T.; Kamigaito, M.; Sawamoto, M. *Macromolecules* **2007**, *40*, 3581−3588.
(28) Zhao, B.; Li, D.; Hua, F.; Green, D. R. *Macromolecules* **2005**, *38*, 9509−9517.
(29) Lutz, J.-F.; Akdemir, O.; Hoth, A. *J. Am. Chem. Soc.* **2006**, *128*, 13046−13047.
(30) Lutz, J.-F.; Weichenhan, K.; Akdemir, O.; Hoth, A. *Macromolecules* **2007**, *40*, 2503−2508.
(31) Jonas, A. M.; Glinel, K.; Oren, R.; Nysten, B.; Huck, W. T. S. *Macromolecules* **2007**, *40*, 4403−4405.
(32) (a) Bhattacharya, A.; Misra, B. N. *Prog. Polym. Sci.* **2004**, *29*, 767−814. (b) Hirao, A.; Hayashi, M.; Loykulnant, S.; Sugiyama, K.; Ryu, S. W.; Haraguchi, N.; Matsuo, A.; Higashihara, T. *Prog. Polym. Sci.* **2005**, *30*, 111−182. (c) Hadjichristidis, N.; Iatrou, H.; Pitsikalis, M.; Mays, J. *Prog. Polym. Sci.* **2006**, *31*, 1068−1132. (d) Yagci, Y.; Tasdelen, M. A. *Prog. Polym. Sci.* **2006**, *31*, 1133−1170. (e) Shinoda, H.; Miller, P. J.; Matyjaszewski, K. *Macromolecules* **2001**, *34*, 3186−3192.
(33) Zhang, M.; Mueller, A. H. E. *J. Polym. Sci., Part A: Polym. Chem.* **2005**, *43*, 3461−3481.
(34) Fischer, K.; Schmidt, M. *Macromol. Rapid Commun.* **2001**, *22*, 787−791.
(35) Wang, J.-S.; Matyjaszewski, K. *J. Am. Chem. Soc.* **1995**, *117*, 5614−15.
(36) Matyjaszewski, K.; Xia, J. *Chem. Rev.* **2001**, *101*, 2921−2990.
(37) Kamigaito, M.; Ando, T.; Sawamoto, M. *Chem. Rev.* **2001**, *101*, 3689−3745.
(38) Tsarevsky, N. V.; Matyjaszewski, K. *Chem. Rev.* **2007**, *107*, 2270−2299.
(39) Matyjaszewski, K. *J. Macromol. Sci., Chem.* **1997**, *A34*, 1785−1801.
(40) Matyjaszewski, K. *Prog. Polym. Sci.* **2005**, *30*, 858−875.
(41) Braunecker, W. A.; Matyjaszewski, K. *Prog. Polym. Sci.* **2007**, *32*, 93−146.
(42) Matyjaszewski, K.; Gaynor, S.; Greszta, D.; Mardare, D.; Shigemoto, T. *J. Phys. Org. Chem.* **1995**, *8*, 306−15.
(43) Matyjaszewski, K. *J. Phys. Org. Chem.* **1995**, *8*, 197−207.
(44) Wang, J.-S.; Matyjaszewski, K. *Macromolecules* **1995**, *28*, 7901−10.
(45) Beers, K. L.; Gaynor, S. G.; Matyjaszewski, K.; Sheiko, S. S.; Moeller, M. *Macromolecules* **1998**, *31*, 9413−9415.
(46) Boerner, H. G.; Beers, K.; Matyjaszewski, K.; Sheiko, S. S.; Moeller, M. *Macromolecules* **2001**, *34*, 4375−4383.
(47) Cheng, G.; Boeker, A.; Zhang, M.; Krausch, G.; Mueller, A. H. E. *Macromolecules* **2001**, *34*, 6883−6888.
(48) Ishizu, K.; Yamada, H. *Macromolecules* **2007**, *40*, 3056−3061.
(49) Pietrasik, J.; Sumerlin, B. S.; Lee, R. Y.; Matyjaszewski, K. *Macromol. Chem. Phys.* **2007**, *208*, 30−36.
(50) Li, C.; Gunari, N.; Fischer, K.; Janshoff, A.; Schmidt, M. *Angew. Chem., Int. Ed.* **2004**, *43*, 1101−1104.
(51) Neugebauer, D.; Zhang, Y.; Pakula, T.; Matyjaszewski, K. *Polymer* **2003**, *44*, 6863−6871.
(52) Yamamoto, S.; Pietrasik, J.; Matyjaszewski, K. *J. Polym. Sci., Part A: Polym. Chem.*, in press.

MA701970T